International Journal of Nanomedicine

Dovepress
open access to scientific and medical research

Open Access Full Text Article

ORIGINAL RESEARCH

Local Sustained Chemotherapy of Pancreatic Cancer Using Endoscopic Ultrasound-Guided Injection of Biodegradable Thermo-Sensitive Hydrogel

Dan Yang, Jing Ning, Xiaomin Liao, Haixing Jiang, Shanyu Qin

Department of Gastroenterology, the First Affiliated Hospital of Guangxi Medical University, Nanning, Guangxi, People's Republic of China

Correspondence: Shanyu Qin, Department of Gastroenterology, the First Affiliated Hospital of Guangxi Medical University, No. 6. Shuangyong Road, Nanning, Guangxi, 53000, People's Republic of China, Tel +86 139 7711 0511, Email qinshanyu@gxmu.edu.cn

Purpose: Endoscopic ultrasound-guided fine-needle injection (EUS-FNI) offers a promising minimally invasive approach for locally targeted management of advanced pancreatic cancer. However, the efficacy is limited due to the rapid plasma clearance of chemotherapeutic agents. Injectable hydrogels can form drug release depots, which provide a feasible solution for optimizing targeted chemotherapy through EUS-FNI.

Methods: A drug delivery system was developed, consisting of gemcitabine (GEM) and thermo-sensitive hydrogel (PLGA-PEG-PLGA, PPP). The injectability, gel formation ability, biocompatibility and sustained drug delivery properties of PPP hydrogel were verified in vitro and in vivo. The effects of GEM/PPP hydrogel on cell proliferation, invasion, metastasis, and apoptosis were explored through co-culturing with PANC-1 cells. The therapeutic effects of GEM/PPP hydrogel on xenograft mice were compared with those of GEM, ethanol and polidocanol using the precisely targeted EUS-FNI technology. Tumor sections were examined by H&E, Ki-67, and TUNEL staining.

Results: GEM/PPP hydrogel exhibited excellent injectability, biocompatibility, and the capability of sustained drug delivery for up to 7 days by forming a gel triggered by body temperature. It demonstrated the best therapeutic effects, significantly reducing proliferation, invasion and migration of PANC-1 cells while promoting apoptosis. After precise injection using EUS-FNI technology, GEM/PPP hydrogel resulted in a reduction of tumor weight by up to 75.96% and extending the survival period by 14.4 days with negligible adverse effects. Pathological examination revealed no systemic toxicity and significant apoptosis and minimal proliferation as well.

Conclusion: The combination of GEM/PPP hydrogel and EUS-FNI technology provides an optimal approach of precise chemotherapy for pancreatic cancer, builds a bridge for clinical translation of basic research, and brings great hope for innovation of minimally invasive treatment modalities. The first-hand EUS image data obtained in this study also serves as a crucial reference for future clinical trials.

Keywords: drug delivery systems, thermo-sensitive hydrogel, endoscopic ultrasound-guided fine needle injection, pancreatic cancer, translational medical research

Introduction

Pancreatic cancer (PC) is a highly lethal and painful malignancy, with a five-year survival rate of approximately 10%.[1,2] Unfortunately, due to the lack of effective early screening strategies, nearly half of patients are diagnosed with advanced-stage disease.[3] Since treatment options are severely limited in advanced stages or metastatic cancers, chemotherapy remains the primary mode of administration for non-resectable patients in the majority of cases.[4,5] However, conventional systemic chemotherapy often fails to produce satisfactory results in clinical practice due to the untargeted delivery of chemotherapeutic agents and significant adverse effects.[6,7] Gemcitabine (GEM) has served as the foundation of PC chemotherapy for over two decades, especially in advanced stage patients with poor health conditions.[8] Nevertheless, its therapeutic benefits are limited due to the rapid plasma elimination with an average half-life of 13.7 minutes.[9] Attempts to achieve more effective local concentrations by increasing drug dosage may result in severe myelosuppression.[9] Additionally, compared to other cancers, PC presents unique hypovascularity and extensive matrix proliferation, making

Received: 5 May 2023
Accepted: 8 July 2023
Published: 20 July 2023

it much more challenging to achieve adequate drug accumulation within the tumor through blood circulation.[10–12] Matrix plays a critical role in inducing drug resistance by hindering the transmission of GEM in PC.[13,14] Hence, novel therapeutic strategies are urgently required to enhance chemotherapy's effectiveness while reducing systemic adverse effects.

Local targeted chemotherapy provides the potential to overcome these limitations of systemic chemotherapy by delivering drugs directly into the tumor microenvironment, thus allowing high local drug concentrations while simultaneously avoiding the side effects caused by non-targeted distribution.[15,16] Currently, the main interventional technologies for local targeted therapy of PC are percutaneous approaches, such as radiofrequency ablation, irreversible electroporation, microwave ablation, cryoablation, and brachytherapy.[17] However, due to the pancreas's deep anatomical location, these percutaneous interventions are prone to severe complications, including pancreatic fistula and bleeding. Endoscopic ultrasound (EUS) can provide better visualization of the pancreatic structure and help reduce the incidence of such complications. Specifically, EUS-guided fine needle injection (EUS-FNI) has been regarded as a feasible and minimally invasive interventional option for local management of PC.[18] In 2016, a study demonstrated that EUS-guided intramural injection of GEM is feasible and potentially effective for treating locally advanced PC.[19] However, benefits were limited because of the rapid clearance of GEM and the advanced stage of cancer in patients. To address the challenge of treatment dilemma, drug nanocarriers have been developed. These nanocarriers provide enhanced anti-cancer effects through active and passive targeting modes.[20,21] Active targeting allows for the recognition of target tumor cells, while passive targeting enhances drug permeation and retention at the tumor site. Local drug nanocarriers, including hydrogels, microspheres, nanoparticles, micelles, and drug-eluting devices, have attracted considerable attention.[22–26] These materials enable effective local drug delivery, reducing the required drug dosage and frequency of administration but still achieve the same therapeutic efficacy, thereby minimizing systemic toxicity and preventing the development of drug resistance due to repeated dosing.[27,28] Among these approaches, smart hydrogels, especially biodegradable thermo-sensitive in situ forming hydrogels, have garnered particular attention. Thermo-sensitive hydrogels are three-dimensional networks composed of hydrophilic copolymers and are popular due to their biocompatibility, biodegradability, drug-loading capacity, and controlled drug release property.[29] These smart hydrogels can modulate drug release by altering their swelling capacity and physical property in response to external stimuli such as body temperature.[30] They are potential candidates for local sustained drug delivery systems in the treatment of PC.[31,32] They can be minimally invasive administered into the tumor site to achieve controlled delivery of therapeutic agents. Upon injection, the drug-loading hydrogel undergoes a solution-gel phase transition triggered by body temperature, resulting in the formation of a semi-solid gel that functions as a drug depot, ensuring sustained release of therapeutic agents over a prolonged period.[33] The well-established interventional EUS-FNI technology enables the precise and safe administration of therapeutic drugs into pancreas.[34] Therefore, the combination of EUS-FNI with sustained drug delivery systems based on injectable thermo-sensitive hydrogel, allowing real-time monitoring during the delivery process, holds great promise as a minimally invasive approach. This clinical translation has significant practical implications for advancing interventional treatment of PC.

Poly(D,L-lactide-co-glycolide) (PLGA)-poly(ethylene glycol) (PEG)-poly(D,L-lactide-co-glycolide) (PLGA) hydrogels are a type of biodegradable and non-toxic triblock copolymer. Both the PLGA and PEG components are approved by the Food and Drug Administration (FDA) for clinical application.[35] Owing to their hydrophilic PEG and hydrophobic PLGA structures, PLGA-PEG-PLGA (PPP) hydrogels have the ability to accommodate both hydrophilic and hydrophobic drugs.[36] Adjusting the composition ratio of PLGA and PEG can modify its drug release duration, enabling precise customizability of chemotherapy.[37] These hydrogels exist in a solution state at room temperature but transition rapidly into a gel once the ambient temperature exceeds the phase transition point, which is typically body temperature.[38] This phase transition property facilitates injection administration without clogging needles. The hydrogel remains in the solution state at lower temperatures, and phase transition occurs at body temperature following injection without requiring external stimuli or supplementary equipment. PPP hydrogel can achieve controlled local chemotherapy without causing serious complications, and do not add systemic toxicity when combined with systemic therapy, which is particularly important for patients with advanced tumor. Compared to other types of hydrogels, PPP hydrogels have several advantages, such as being cost-effective solution, having higher capacity, easier accessibility, and greater commercial availability, making them promising for local drug delivery.[35]

Herein, we have developed a biodegradable and thermo-sensitive drug delivery system that enables precise and controlled chemotherapy through EUS-FNI technology, resulting in sustained release of chemotherapeutic agents within the tumor, as shown in Scheme 1. This system is composed of GEM, the first-line drug for PC monotherapy, and PPP hydrogel. Through a series of in vitro and in vivo analyses, we meticulously evaluated the clinical feasibility and sustained drug release properties of this system. In conjunction with EUS-FNI technology, we were the first to administer GEM/PPP hydrogel for injection directly to xenograft models of PC using a fine needle under ultrasound guidance. We not only explored the anti-tumor effect of the system, but also obtained real-time EUS image data, and this provided a valuable reference for the clinical application of the system. Furthermore, we compared the anti-tumor effect of this system to classic chemical ablative drugs, providing additional significant evidence for clinical application.

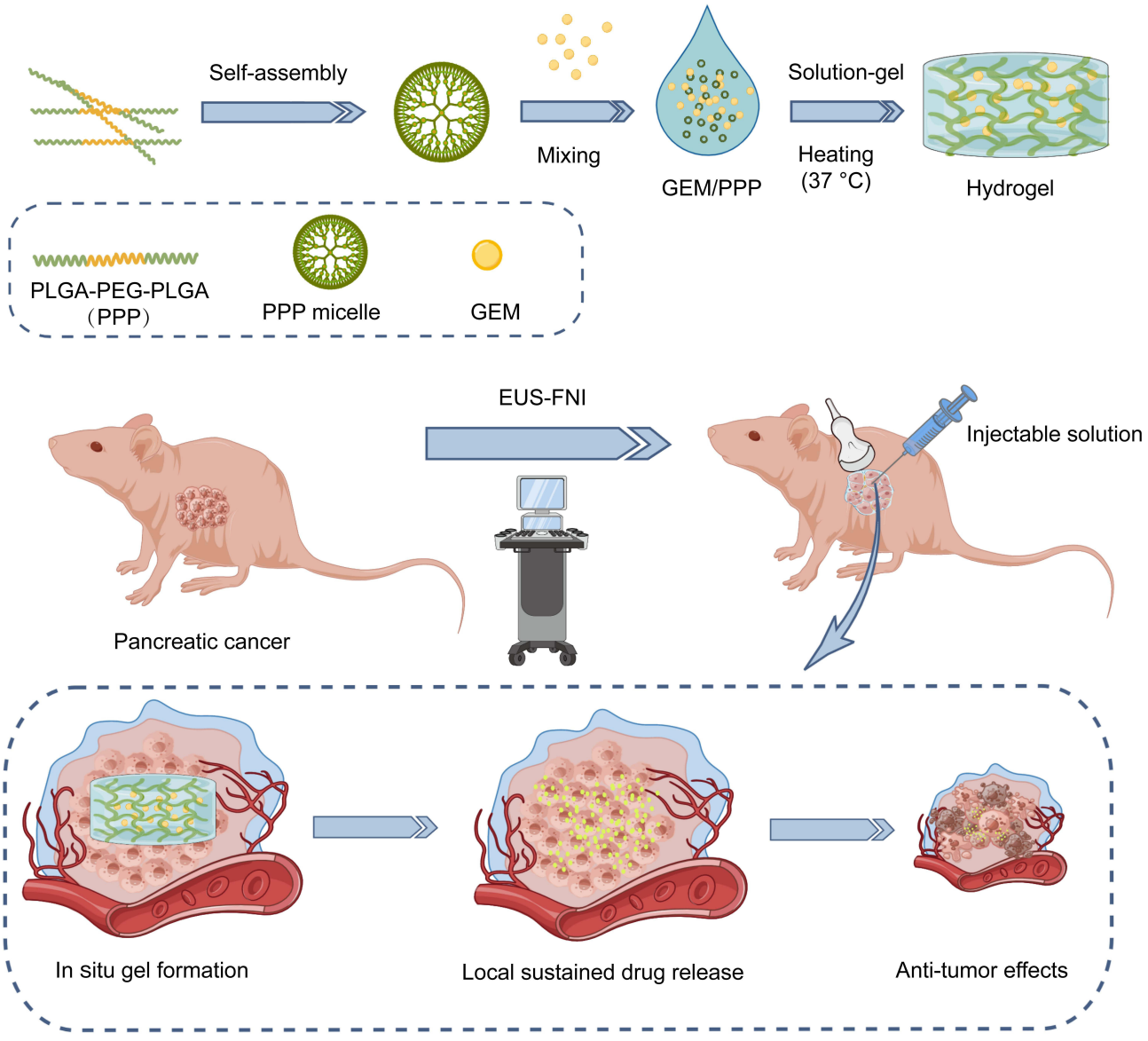

Scheme 1 Schematic representation of the sustained delivery of gemcitabine (GEM) through a biodegradable thermo-sensitive hydrogel (PLGA-PEG-PLGA, PPP). This injectable hydrogel allows for direct administration into pancreatic cancer via endoscopic ultrasound-guided fine needle injection (EUS-FNI) and facilitates sustained local drug delivery of GEM to exert an anti-tumor effect.

Materials and Methods

Materials

PLGA75/25(1740)-PEG(1500)-PLGA75/25(1740) was purchased from MELOPEG (Shanghai, China). Gemcitabine hydrochloride (99%) was purchased from MedChemExpress (New Jersey, USA). Ethanol (98%) was purchased from SINOPHARM (Anhui, China). Polidocanol was purchased from GlpBio (California, USA). Cyanine 5.5 N-hydroxysuccinimide (Cy5.5 NHS) ester was purchased from APExBIO (Houston, USA). Dulbecco's Modified Eagle Medium (DMEM) and fetal bovine serum (FBS) were from Gibco (Maryland, USA). Cell Counting Kit-8 (CCK-8) was purchased from Meilunbio (Dalian, China). *Transwell* Insert and *Matrigel* matrix were purchased from Corning (New York, USA). Annexin V-Fluorescein Isothiocyanate/Propidium Iodide (FITC/PI) apoptosis detection kit and Penicillin-Streptomycin-Amphotericin B liquid were purchased from Solarbio (Beijing, China). Terminal deoxynucleotidyl transferase dUTP Nick End Labeling (TUNEL) apoptosis kit was purchased from MULTI SCIENCES (Hangzhou, China). Proliferation marker protein Ki-67 was purchased from Servicebio (Wuhan, China).

Preparation of GEM/PPP Hydrogel

To form the micelle through self-assembly, the PPP hydrogel was dissolved in phosphate-buffered saline (PBS, pH 7.4). Then, a homogeneous solution of GEM/PPP hydrogel was prepared at room temperature by dissolving a predetermined quantity of GEM in the PPP hydrogel solution. PPP hydrogels with concentrations of 15, 20, and 25 wt.% were prepared, and the one exhibiting a phase transition temperature closest to body temperature was selected. All samples underwent sterilization using a 0.22 μm filter membrane.

Phase Diagram Measurement

To investigate the thermo-sensitive solution-gel phase transition of PPP and GEM/PPP hydrogel, the tube-inverting method was used. Samples of different concentrations (0.5 mL each) were placed in test tubes and incubated from room temperature, increasing the temperature to the precipitation temperature at 1°C intervals. The gel was considered to have formed when the sample vial did not exhibit observable flow within 1 minute after being inverted. The injectability and instant gelation behavior of GEM/PPP hydrogels were evaluated using a 1 mL syringe at room temperature and in a water bath at 37 °C.

Degradation Studies in vitro and in vivo

The GEM/PPP hydrogel (PPP: 20 wt.%, GEM: 10mg/mL) was formed and stabilized in culture dish at 37°C. Subsequently, the hydrogel was incubated in pre-warmed PBS (37°C) for 4 weeks. To measure the rate of degradation, residual PBS was aspirated from the culture dish every two days, followed by precise measurement of the weight of the remaining hydrogel. In vivo biodegradation of the GEM/PPP hydrogel was observed in BALB/c nude mice (n=3). A 200 μL solution of PPP hydrogel was subcutaneously injected via a 30-gauge needle, and the degradation was observed at 0–4 weeks post-injection. Cy5.5 was used as an alternative to GEM, and the blue color facilitated the visualization of biodegradation in vivo. The Animal Care & Welfare Committee of Guangxi Medical University approved all animal experiments (NO.202212003).

Drug Release in vitro

To investigate the release kinetics of GEM from PPP hydrogel in vitro, 1 mL of GEM loading hydrogel solution was added to the bottom of Eppendorf tubes and incubated under gentle shaking (50 rpm) at 37 °C in PBS (pH 7.4 and pH 5.0). The supernatant was collected at predetermined time intervals, and its concentration of released GEM was determined by high-performance liquid chromatography (HPLC). A reversed-phase C18 column (4.6 mm × 250 mm, 5 μm, SHIMADZU LC-20AB, Kyoto, Japan) was used for detection at a wavelength of 243 nm. The mobile phase, comprising a 0.1% trifluoroacetic acid aqueous solution and methanol (90:10, v/v), was delivered at a flow rate of 1 mL/min.

Drug Release in vivo

To evaluate the distribution and persistence of drug-loading hydrogel composites in vivo, two groups of nude mice (n=3) were subcutaneously injected with 100 μL of either Cy5.5 solution in normal saline or Cy5.5/PPP hydrogel. Fluorescence images were captured at pre-determined time points using a multimodal animal in vivo imaging system (BLT AV100, Guangzhou, China; excitation = 675 nm, emission = 693 nm) after anesthetizing the mice with isoflurane (RWD, Shenzhen, China). The images were analyzed using AniView software (v1.00.0049).

Cytotoxicity in vitro

The cytotoxicity of GEM against Pancreatic carcinoma-1 (PANC-1) cells was assessed by conducting the CCK-8 assay. PANC-1 cells were purchased from the Procell Life Science&Technology (Wuhan, China), and cultured in DMEM supplemented with 10% FBS and 1% Penicillin-Streptomycin-Amphotericin B liquid as recommended. 100 μL of cell suspension (4500 cells) was added to each well of a 96-well plate and incubated for 24 hours. Next, the original medium was replaced with 100 μL of fresh medium containing GEM at different concentrations (n=5). Cells were cultured for another 48 hours before performing the CCK-8 assay, measuring absorbance at 450 nm with a microplate reader (Synergy H1, Biotek, Vermont, USA). The half maximal inhibitory concentration (IC50) was calculated using ImageJ software.

The in vitro anti-tumor activity of GEM/PPP hydrogel was evaluated using a 24-well Transwell co-culture system (n = 3). First, 500 μL of PANC-1 cell suspension (10,000 cells) was added to the lower chambers of the Transwell and cultured for 24 hours. Next, 50 μL of PBS, GEM (50 μM) or PPP hydrogel (20 wt.%) was added to the upper chamber of the Transwell. To create a drug depot, GEM/PPP hydrogel (50 μM GEM) was also pipetted to the upper chamber of the Transwell. All hydrogels were kept at 37 °C for 30 min to form stable gels before co-culturing with PANC-1 cells. After co-culturing for 24 hours, all formulations were replaced with fresh medium to refresh the culture conditions. After incubation for 24, 48, and 72 hours, cell viability was assessed using the CCK-8 assay, and optical density (OD) values at 450 nm were measured.

Effects on Cell Migration and Invasion Capacity in vitro

To assess the migration capacity of PANC-1 cells, a wound healing assay was performed in 6-well Transwell co-culture system. Each well was seeded with 100,000 cells. After manual scratching of the cell monolayer, the wells were rinsed with PBS and incubated with 2 mL fresh serum-free medium. Then, 200 μL of PBS, PPP hydrogel, GEM, or GEM/PPP hydrogel was pipetted into the upper chamber. The scratch area was photographed at 0, 24 and 48 hours, and the distance migrated by the cells was measured using ImageJ software. The cell migration rate was calculated using the formula: (0-hour scratch width - 24 or 48-hour scratch width) / 0-hour scratch width.

For the invasion assay, a 24-well Transwell system with a pore size of 8.0 μm was used. The upper chamber was filled with 100,000 cells suspended in 200 μL serum-free medium and Matrigel (30 μL) was added to coat the surface of the Transwell membrane. In the lower chamber, 50 μL of one of the following solutions was added: PBS, PPP hydrogel, GEM, or GEM/PPP hydrogel, along with 500 μL of DMEM containing 20% FBS. After 24 hours of incubation, non-invading cells were removed from the upper surface of the insert with a wet cotton swab. The lower surface of the insert was fixed with 4% paraformaldehyde for 30 minutes and subsequently stained with 0.2% crystal violet for 20 minutes. Migration experiments were performed using the same 24-well Transwell system, but with some modifications. No Matrigel was added to the upper chamber, and a lower cell density of 10,000 cells/well was seeded. The number of cells that migrated through the membrane was counted using ImageJ software.

Cell Apoptosis Analysis in vitro

Flow cytometry analysis was conducted to evaluate apoptosis in PANC-1 cells after incubation. The co-culture system described in the previous section was used. After 48 hours of incubation, cells were collected and stained with Annexin V-FITC/PI according to the manufacturer's protocol. The fluorescence of cells was analyzed using a flow cytometer (BD FACSCalibur, New Jersey, USA), and the data were processed with FlowJo 7.6.1 software. To observe the fluorescent

morphology of PANC-1 cells, images were captured using a digital inverted fluorescence microscope (EVOS® FL, Thermo Fisher Scientific, Tokyo, Japan).

Anti-Tumor Experiments in vivo via EUS-FNI

A two-step tissue block graft method was utilized to establish xenograft models. PANC-1 cells (1×10^7 cells) suspended in 100 μL of DMEM without FBS were subcutaneously injected into the right axillary area of female BALB/c nude mice (20 ± 2 g). Once the tumors grew to 800–1000 mm^3, they were excised and cut into small tissue fragments measuring 2 mm^3. Then these tissue fragments were transplanted into the same position in other mice using a trocar. Tumor volume was calculated using the following equation: volume = length × $width^2$ / 2.

Once the tumor volume had reached approximately 500 mm^3, the xenograft mice were randomly divided into six groups (n=10) and subjected to different treatments via either intratumoral injection (i.t.) or intravenous injection (i.v.). The intervention measures included normal saline (NS) (i.t.), GEM (i.v.), GEM (i.t.), GEM/PPP hydrogel (i.t.), ethanol (i.t.), and polidocanol (i.t.). The entire treatment process was precisely guided by an animal ultrasound instrument (Esaote MyLab X6, Italy), and monitored in real-time. The mice were anesthetized with isoflurane. The dose of GEM was maintained at 30 mg/kg. The ethanol concentration was 98%, and the polidocanol concentration was 10 mg/mL. Tumor size and mice weight was assessed every two days. On day 25 after treatment, half of the mice were euthanized, and their tumors, as well as major organs including the heart, liver, spleen, lungs, and kidneys, were collected. The size and weight of the tumors were measured, and all specimens were fixed in 4% paraformaldehyde for further examination. The remaining mice (n=5) were continuously monitored for survival analysis.

Pathomorphological Examination

The fixed tumors and major organs were dehydrated through ethanol, embedded in paraffin, and then cut into slices to be evaluated histologically via hematoxylin-eosin (H&E) staining. Ki-67 and TUNEL staining were performed to investigate cancer cell proliferation and apoptosis in the tumor tissue. All stained slices were observed under a fluorescence microscope manufactured by Olympus in Tokyo, Japan. The positive ratio of Ki-67 and TUNEL staining was measured by ImageJ software.

Statistical Analysis

All experiments were conducted with three independent replicates. The results were analyzed using SPSS 25.0 software. Normally distributed data were analyzed by one-way ANOVA, and presented as mean ± standard deviation (SD). Non-normally distributed data were analyzed by non-parametric tests, and presented as median and 95% confidence interval (CI). Additionally, survival benefits were evaluated through log-rank survival analysis. $P<0.05$ were considered statistically significant, and these significance levels were indicated with an asterisk (*$P < 0.05$, **$P < 0.01$, ***$P < 0.001$).

Results and Discussion

Solution–Gel Phase Transition Behavior

PPP hydrogel is a homogeneous micellar solution at 25°C that can be easily mixed with drugs. By utilizing the liquid form of PPP hydrogel at room temperature, we prepared drug-loading hydrogel through simple mixing of the two components. The synthesized GEM/PPP hydrogel contained 10 mg/mL of GEM. We tested the phase transition temperatures of GEM/PPP hydrogel at concentrations of 15 wt.%, 20 wt.%, and 25 wt.%, and found that adding GEM resulted in a slight increase in the phase transition temperature of PPP hydrogel (Figure 1A). Hydrogel at 20 wt.% concentration had a phase transition temperature of 37.3°C, which is closest to the physiological temperature. The phase transition temperature near body temperature allows the gel to form in situ without additional stimuli.[39] During sterilization of the hydrogels, we noticed that higher concentrations of hydrogel resulted in greater volume loss during filtration. Furthermore, higher concentrations increased the risk of needle clogging. Therefore, we chose 20 wt.% for subsequent assessments. This concentration exhibited excellent flowability and underwent a solution-gel transition at a desirable temperature of 37°C (Figure 1B). To confirm the suitability of GEM/PPP hydrogel for fine needle delivery,

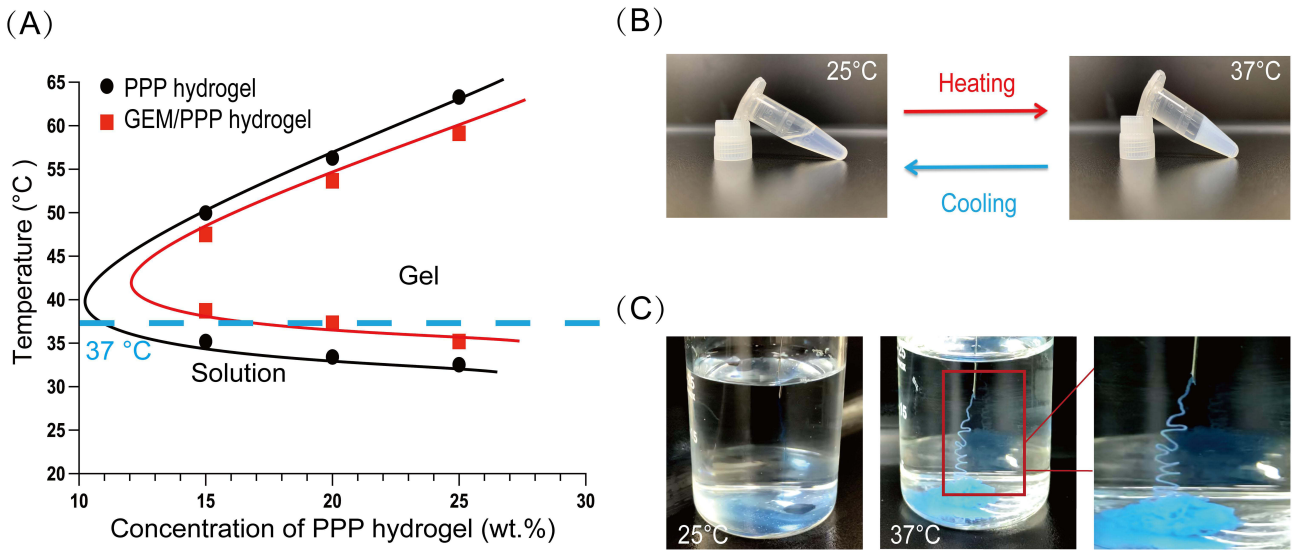

Figure 1 The solution-gel phase transition behavior. (**A**) Changes in the phase transition temperature of PPP hydrogel and GEM/PPP hydrogel with different concentrations of PPP copolymer. The blue dashed line corresponds to 37 °C. (**B**) Reversible solution-gel phase transition of GEM/PPP hydrogel (polymer concentration: 20 wt.%; GEM loading amount: 10 mg/mL) between 25 °C and 37 °C. (**C**) Injectability and rapid in situ gelation ability of GEM/PPP hydrogel (stained by Cy5.5). All data were obtained with 3 independent repeated experiments and presented as mean ± SD.

we assessed its injectability and in situ gelation. Needle blockage and pre-gelation in needle tubing could severely limit its clinical application. The results showed that the hydrogel could be injected smoothly using a fine needle at 25°C without any issues of syringe clogging (Figure 1C). Upon injection into warm water at 37°C, we observed instant gelation and stable gel maintenance, further demonstrating the feasibility of GEM/PPP hydrogel in EUS-FNI.

Degradation in vitro and in vivo

The GEM/PPP hydrogel maintained its integrity in vitro for up to 21 days, after which the gel skeleton collapsed, leaving only a small amount of hydrogel matrix by day 28. Continuous weight measurement of GEM/PPP hydrogel displayed that it absorbed water and swelled in the early stage (2–5 days), peaking on day 3 with more than double the original weight, then decreasing (Figure 2A). The hydrogel's polymer network, incorporating hydrophilic PEG moieties, facilitates water absorption and contributes to its initial swelling, accounting for the weight gain observed at early stage. Then the degradation of PLGA crosslinks leads to the dissolution of PEG molecules, resulting in the sharp decrease after reaching the peak.[40]

Biocompatibility is a fundamental requirement for drug delivery materials. It requires the materials should have no significant adverse effects like chronic inflammation, tissue hyperplasia, immune rejection and carcinogenesis.[41] This demands the hydrogel itself, including its degradation products, are non-toxic and biodegradable. To evaluate its biocompatibility as a drug delivery material, we subcutaneously injected a solution of the PPP hydrogel solution (stained by Cy5.5) into Balb/c nude mice. This resulted in the rapid formation of a blue, round hydrogel at the injection site, which gradually decreased in size and color over time (Figure 2B). The hydrogel remained in vivo for around 28 days, with the most notable degradation rate occurring during the first week (Figure 2C). No adverse effects, such as weight loss, skin and surrounding tissue inflammation, were observed in mice during this process. This represents that PPP hydrogel has a good biocompatibility.

Drug Release Profiles

The interconnecting networks of PPP hydrogel lay the foundation for drug entrapment. Once a stable gel is formed, the hydrogel's porous structure provides sustained release capacity.[42] Given the acidic tumor microenvironment in PC as a result of hypovascularity and hypoperfusion, characterized by hyperfibrosis and limited oxygen and nutrient supply, we investigated the in vitro drug release profile of GEM loaded in PPP hydrogel under the neutral and acidic PBS solution.[43]

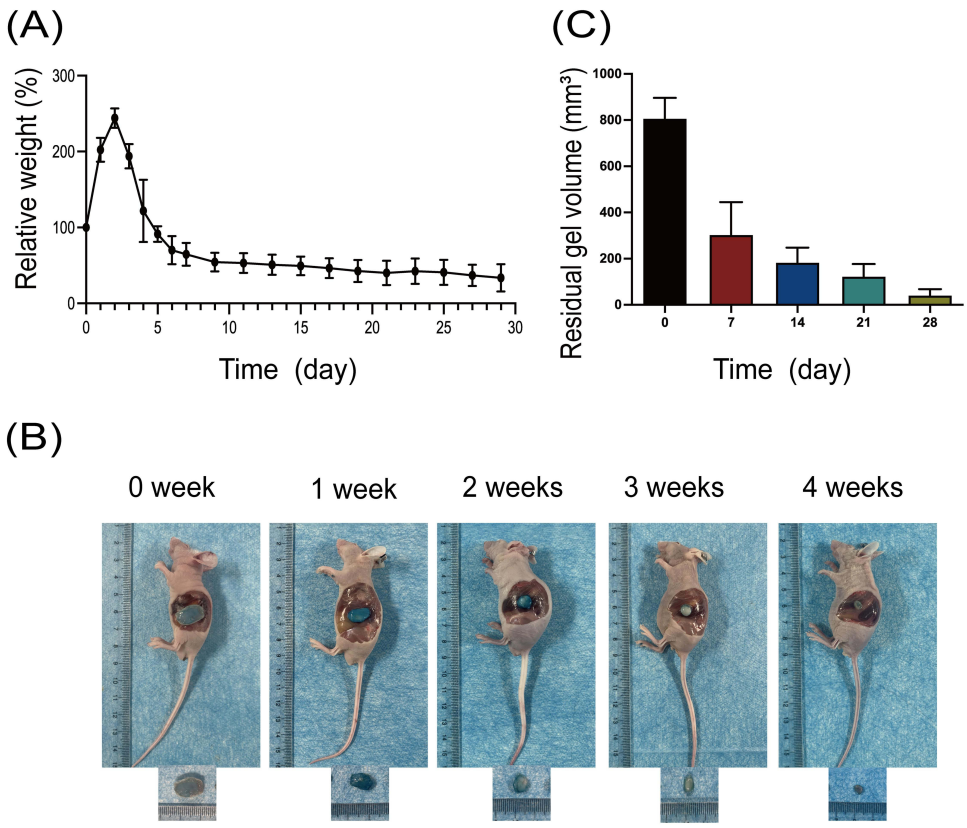

Figure 2 Degradation of GEM/PPP hydrogel in vitro and in vivo. (**A**) In vitro degradability of GEM/PPP hydrogel. (**B**) In vivo biodegradability of GEM/PPP hydrogel (stained by Cy5.5). (**C**) Residual gel volume in nude mice. Relative weight is a ratio of weight measured at a preset time point to the first day. All data were obtained with 3 independent repeated experiments and presented as mean ± SD.

Our findings demonstrated a typical two-stage release pattern observed in hydrogels.[44] Specifically, an initial burst release was observed within the first 24 hours, followed by a sustained and gradual release over time (Figure 3A). During the first stage, GEM was released at a nearly constant rate, which gradually slowed down during the second stage. Notably, while the PPP hydrogel is not pH-sensitive, the acidic microenvironment still reduced its first-stage release rate. Under neutral conditions, the cumulative release percentage of GEM was 75.98% over 48 hours and 85.49% after 7 days, compared to 63.83% and 79.51%, respectively, under acidic conditions. A similar phenomenon has been previously reported in GEM-loaded PLGA nanoparticles.[45] Decrease in pH resulted in a flatter cumulative release curve, but regardless of the pH level in the micorenvironment, the PLGA nanoparticles possessed sustained drug release capabilities. Our results confirm that this phenomenon is also present in PPP hydrogel.

Furthermore, an in vivo imaging system was utilized to investigate the drug retention after delivery by the PPP hydrogel. By using the water-soluble fluorescent dye Cy5.5 as a surrogate for GEM, we simulated the retention and distribution of the drug in vivo and tracked its intensity in real-time. After subcutaneously administered, Cy5.5 was absorbed by the surrounding tissues, and circulated throughout the body via blood circulation, with the most pronounced fluorescence intensity in vascular-rich organs like heart, lungs, and brain (Figures 3B). The fluorescence intensity of mice treated with Cy5.5 solution exhibited a rapid decline within 24 hours and reached almost undetectable levels by 72 hours (Figure 3C). In contrast, administration of Cy5.5 via the PPP hydrogel showed a significantly slower decay in fluorescence intensity, with strong fluorescence still detectable even after 168 hours post-administration.These results demonstrate that the PPP hydrogel is a reliable material for sustained drug release, guaranteeing the continuous release of drugs for over 7 days in vitro and in vivo. Considering that GEM has a plasma half-life of only 13.7 minutes, utilizing the PPP hydrogel significantly prolongs the drug's duration of action.[9] It is worth mentioning that the degree of swelling and

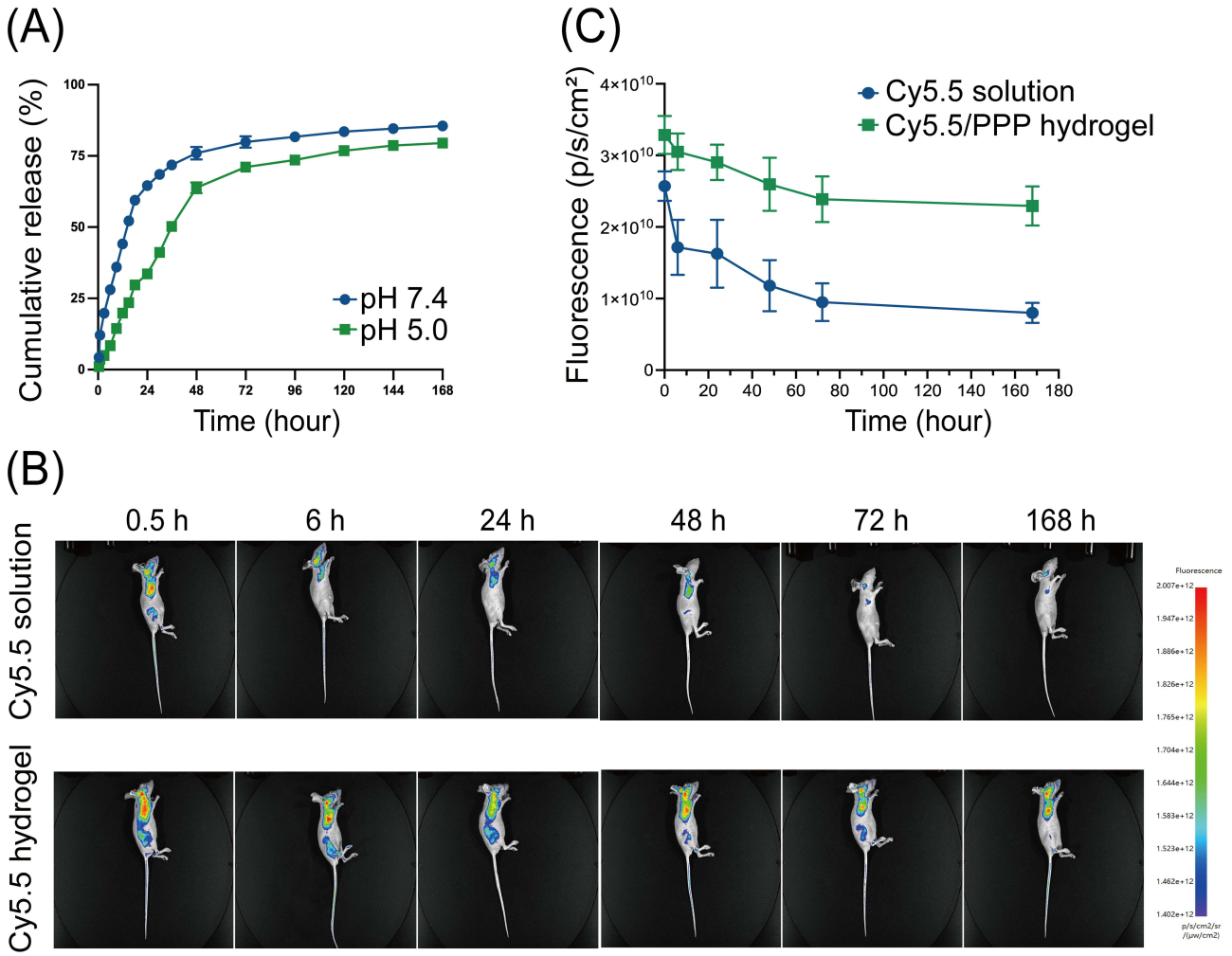

Figure 3 Drug release of GEM/PPP hydrogel in vitro and in vivo. (**A**) Cumulative amounts of GEM were released from GEM/PPP hydrogel at different pH conditions (pH 7.4 and 5.0). (**B**) Real-time in vivo fluorescent imaging of nude mice with subcutaneous injection of Cy5.5 solution or Cy5.5/PPP hydrogel. All images shown in the same group were from the same mouse. (**C**) The fluorescence intensity of mice. All data were obtained with 3 independent repeated experiments and presented as mean ± SD.

pore size of PPP hydrogel can be modulated by adjusting the composition ratio of PLGA and PEG, allowing for personalized chemotherapy.[37] The use of PPP hydrogel may offer enhanced prospects for advanced PC patients.

Anti-Tumor Effects in vitro

We conducted a series of experiments to assess the in vitro anti-tumor therapeutic efficacy of GEM/PPP hydrogel. The anti-tumor effect of GEM on PANC-1 cells was demonstrated to be time and concentration-dependent using CCK-8 assays. After 48 hours of incubation, the IC50 value of GEM was calculated as 5.717 μM. As depicted in Figure 4A, we employed the Transwell co-culture system to simulate sustained drug release. Since the drug concentration in the co-culture system was diluted tenfold, we chose a GEM concentration of 50 μM for subsequent experiments. To mimic its rapid plasma clearance, the initial medium in the Transwell system was replaced with fresh medium after a incubation of 24 hours.

It was observed that the blank PPP hydrogel exhibited favorable biosafety, and allowed for high cellular viability of PANC-1 cells in a series of experiments, consistent with those reported in the literature.[35] GEM/PPP hydrogel demonstrated superior inhibition of cell proliferation compared to GEM at 24, 48, and 72 hours (Figure 4B). Notably, the viability of PANC-1 cells in the free GEM restored after replacing the initial medium with fresh medium at 24 hours. On the other hand, GEM/PPP hydrogel showed consistent cytotoxicity, with cell viability remaining at only 34.75% of the

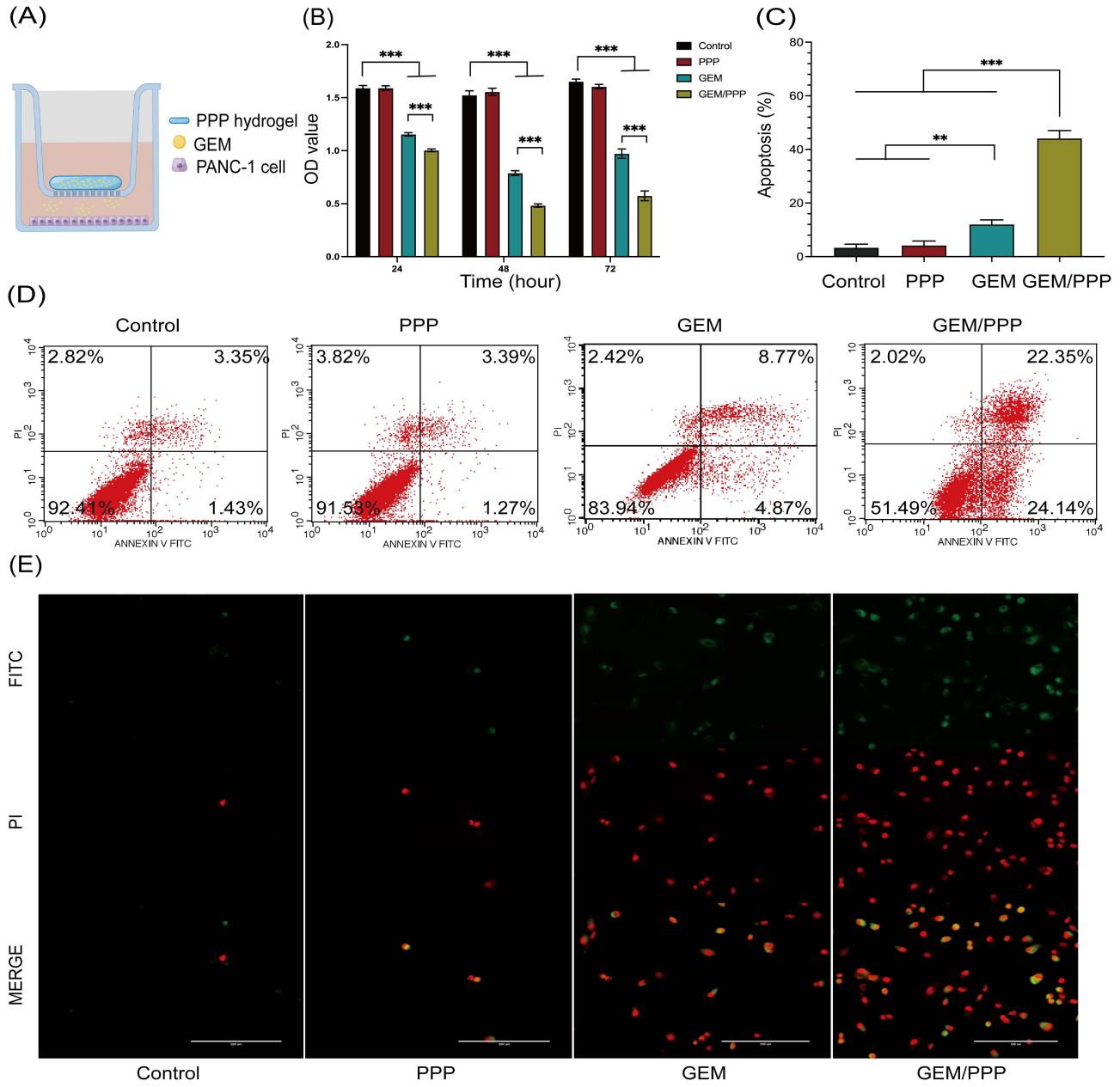

Figure 4 Cell viability and apoptosis of PANC-1 cells in vitro. (**A**) Schematic illustration of the Transwell co-culture system used to create a drug depot. (**B**) Cell viability of PANC-I cells incubated in the Transwell co-culture system was evaluated at 24, 48, and 72 hours. (**C**) Cell apoptosis of PANC-I cells incubated in the Transwell co-culture system was evaluated at 48 hours. (**D**) Cell apoptosis analysis measured by flow cytometry (stained by Annexin V-FITC/PI). (**E**) Representative fluorescent morphology images of the apoptotic PANC-1 cells were obtained after 48 hours of co-cultivation. Double-stained cells represent apoptotic cells. Scale bar is 200 μm. All data were obtained through three independent repeated experiments and presented as the mean ± SD. A significant difference was observed in the LSD post-hoc test. ***$P < 0.001$, **$P < 0.01$.

blank control group at 72 hours. The results of apoptosis were concordant with those obtained from the CCK-8 assay, demonstrating that GEM/PPP hydrogel induced the highest level of apoptosis of all (Figures 4C and D). Additionally, fluorescence microscopy also revealed that GEM/PPP hydrogel induced the highest level of apoptosis, as evidenced by largest number of double-stained cells (Figure 4E). All these findings suggest that GEM/PPP hydrogel can effectively inhibit cell proliferation and induce apoptosis in PANC-1 cells.

The results of the wound healing assay showed that PANC-1 cells co-cultured with GEM/PPP hydrogel exhibited the most significant inhibition of cell migration, as evidenced by the lowest migration rate of only 6.83% and 15.86% at 24 and 48 hours respectively (Figures 5A and B), which was significantly lower than those co-cultured with free GEM.

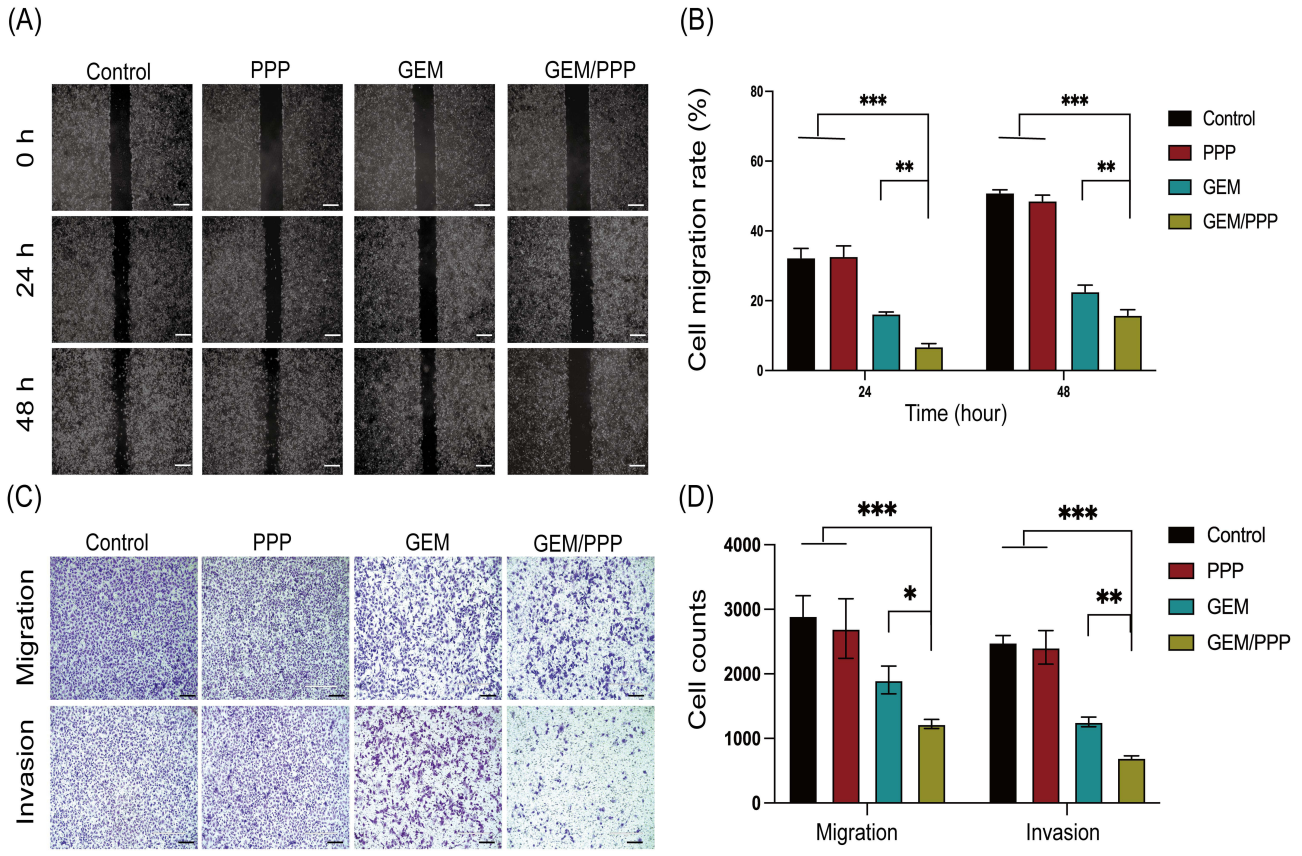

Figure 5 Cell migration and invasion ability of PANC-1 cells in vitro. (**A**) Representative images of wound healing assay at 0h, 24h and 48h. (**B**) The quantitative analysis of wound healing assay. (**C**) Representative images of transwell assay. (**D**) The quantitative analysis of cells that passed the membrane in transwell assay. Scale bar is 200 μm. All data were obtained through three independent repeated experiments and presented as the mean ± SD. A significant difference was observed in the LSD post-hoc test. ***$P < 0.001$, **$P < 0.01$, *$P < 0.05$.

Moreover, the transwell assays demonstrated that the cell migration and invasion ability in the GEM/PPP hydrogel group were only 64.30% and 55.81% of those in the GEM group (Figures 5C and D). These findings suggest that GEM/PPP hydrogel is superior to free GEM in inhibiting the migration and invasion of PANC-1 cells.

The superior effects of GEM/PPP hydrogel are attributed to the sustained drug release from the micellar network within PPP hydrogel. Within the GEM/PPP hydrogel, approximately 60% of the total GEM dose was released due to swelling in the first 24 hours. This initial burst was removed after replacing the culture medium. The remaining drug in GEM/PPP hydrogel was slowly and sustainably released from the micellar network through the dissolution of the hydrogel skeleton, which could last up to 7 days, providing consistent anti-tumor effects. In contrast, the GEM group had all GEM cleared, which simulated real physical conditions. Therefore, regained cell vitality was observed in the GEM group. These results indicate that GEM/PPP hydrogel exhibits stronger cytotoxicity, making it an ideal candidate for optimizing chemotherapy strategies for PC.

Anti-Tumor Effects in vivo via EUS-FNI

Building on the encouraging anti-tumor effects of GEM/PPP hydrogel in vitro, we further investigated its efficacy against tumors in xenograft mice models using precise intratumoral injection guided by EUS (Figure 6A). To our knowledge, this is the first study to combine EUS-FNI technology and drug delivery hydrogel for PC treatment. After injecting GEM solution into the tumor, a hyperechoic mist was diffusely distributed throughout the entire mass (Figure 6B), consistent with previously observed results in human experiments.[19] When injecting GEM/PPP hydrogel, restricted and layered hyperechoic patterns were observed beneath the needle tip, indicating instant gel formation. No needle blockage or liquid extravasation was observed during the injection of hydrogel, demonstrating the feasibility of GEM/PPP hydrogel in EUS-FNI technology.

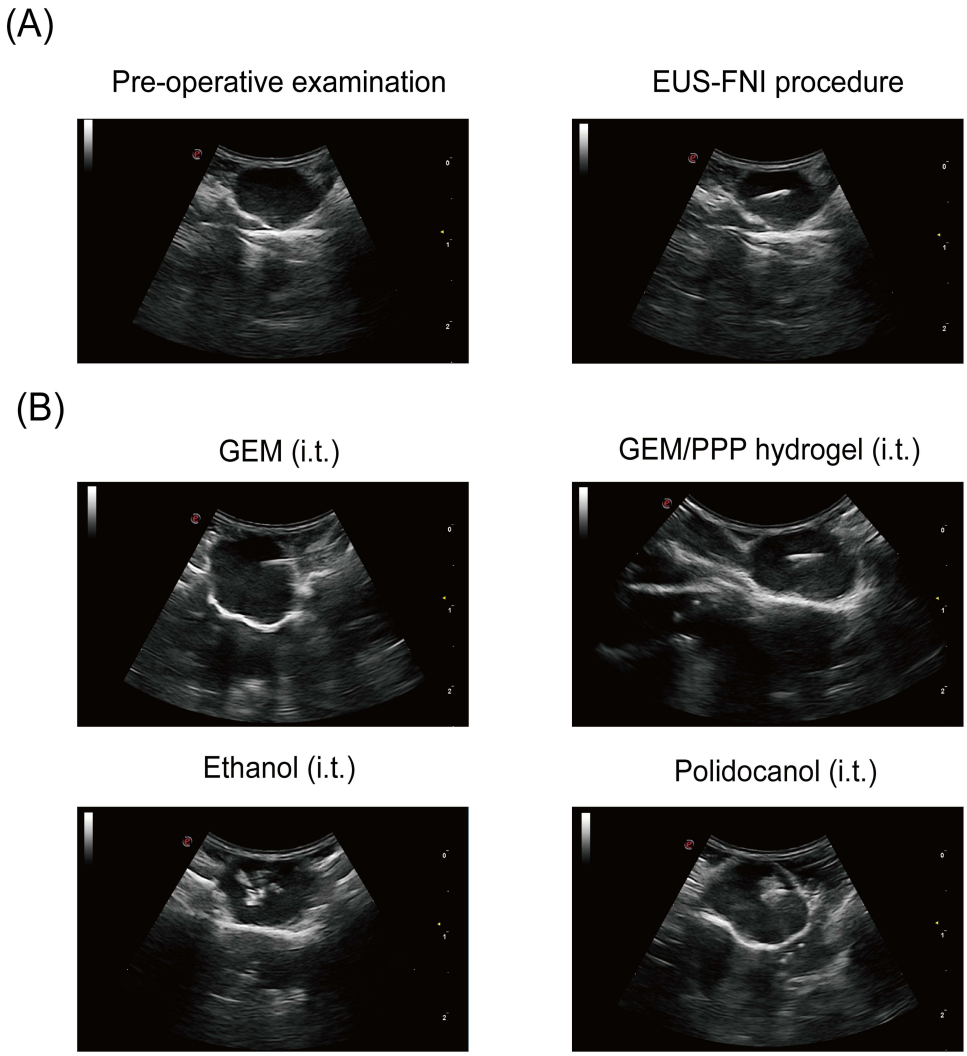

Figure 6 Representative images of EUS-FNI. (**A**) The procedure of real-time EUS-FNI. (**B**) Ultrasonographic images of different formulations during procedure. GEM solution injection resulted in rapid diffusion of a hyperechoic substance throughout the tumor mass. GEM/PPP hydrogel injection produced confined, layered hyperechoic matter near the needle tip. Ethanol injection generated irregularly shaped hyperechoic regions. Polidocanol injection created a limited, spherical hyperechoic area surrounding the needle tip.

Furthermore, ethanol injection produced irregular hyperechoes with petal-shaped morphology and a more extensive distribution than an equivalent volume of polidocanol. In contrast, polidocanol exhibited limited spherical hyperechoes around the needle tip during injection. These results confirm the efficacy of our model in observing the ablation process, treatment outcomes, and serve as a reference for future clinical trials.

After treatment, we evaluated the changes of tumor growth, body weight, and survival status in mice. These results are illustrated in Figure 7. All treatment regimens inhibited tumor growth. Notably, the GEM/PPP hydrogel (i.t.) group exhibited the most significant therapeutic effects, as evidenced by the smallest tumor dimensions and lowest tumor weight (Figure 7A–C). The final tumor weight of the GEM/PPP hydrogel (i.t.) group was only 24.04% of that in the NS (i.t.) group. To assess chemotherapy safety, systemic toxicity was evaluated by changes in body weight and tissue damage. The GEM/PPP hydrogel (i.t.) group had the highest body weights (Figure 7D). These findings suggest that the GEM/PPP hydrogel effectively delivered anti-tumor drugs in a sustained and localized manner without causing obvious systemic toxicity. Worth noting is that the survival time of mice in the GEM/PPP hydrogel (i.t.) group was 42.4 days, which far exceeded the survival time of NS (i.t.) mice, whose survival time was 28 days (Figure 7E).

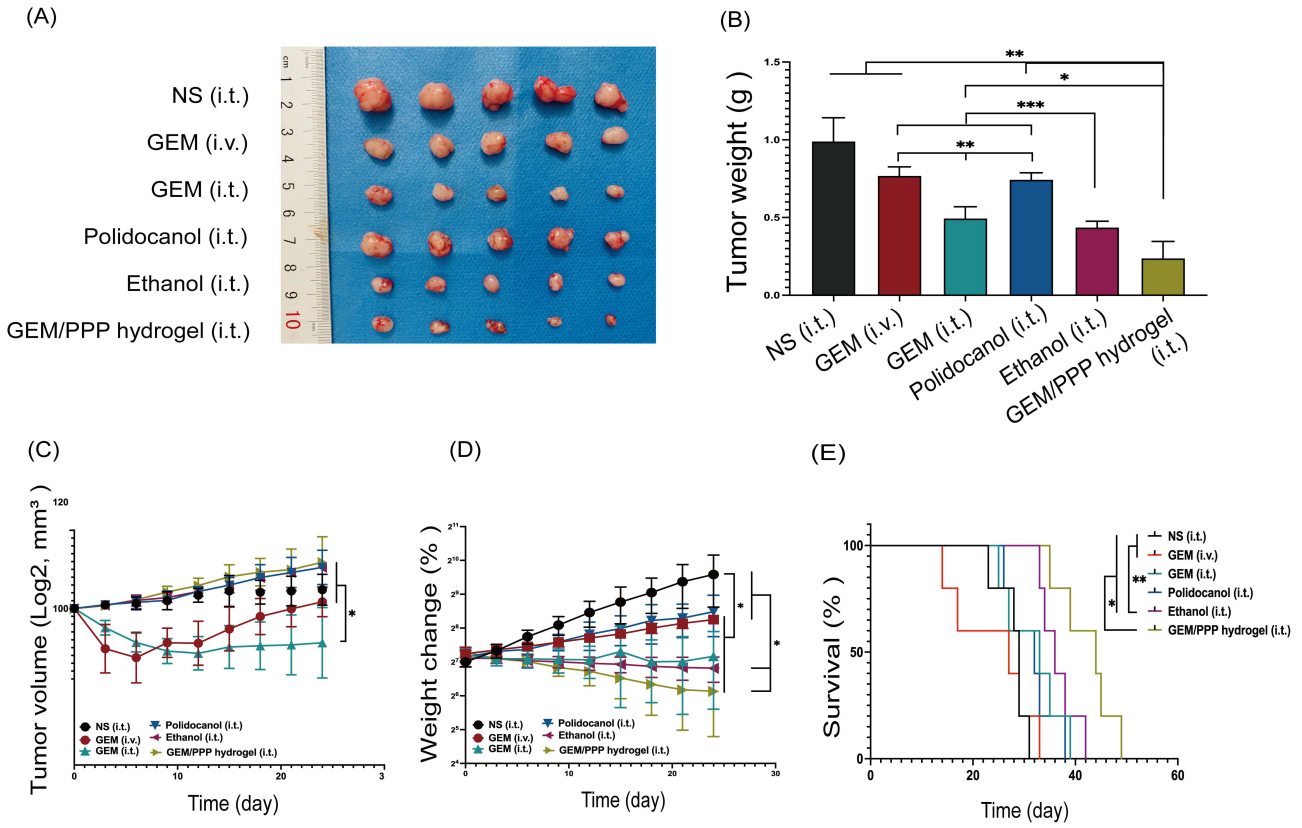

Figure 7 The anti-tumor efficiency of different groups in vivo. (**A**) The photograph of excised tumors on day 25 post-treatment. (**B**) Tumor weight of excised tumors. A significant difference was observed in the Tamhane's T2 test. (**C**) Tumor growth curves of the mice during treatments. A significant difference was observed in the median test. (**D**) Body weight changes curves of the mice during treatments. A significant difference was observed in the LSD post-hoc test. (**E**) Survival curves of mice in different groups. A significant difference was observed in the log-rank survival analysis. ***$P < 0.001$, **$P < 0.01$, *$P < 0.05$.

The GEM (i.t.) group exhibited a more potent anti-tumor effect than the GEM (i.v.) group, as demonstrated by tumor weight. Both intravenous and intratumoral administration of GEM resulted in significant weight loss. Although the GEM (i.v.) group experienced significant initial weight loss, they began to gain weight on day 9 and ultimately outperformed the GEM (i.t.) group. These findings suggested that the tumor matrix limited the ability of GEM to reach an effective drug concentration within the tumor, resulting in better treatment efficacy via intratumoral injection compared to intravenous injection. However, intratumoral administration carried a higher risk of systemic toxicity. Furthermore, intravenous administration of GEM did not confer any survival benefit and yielded the shortest survival time of 24 days. These results indicate that, compared to free GEM, GEM/PPP hydrogel is superior in terms of treatment efficacy, safety, and survival time, regardless of the route of administration.

Ethanol, known as one of the most potent ablative agents, has shown good therapeutic effects for pancreatic lesions.[46] Although the tumor weight of the ethanol (i.t.) group was comparable to the GEM/PPP hydrogel (i.t.) group (P=0.162), its survival time was shorter (P=0.047). However, due to its strong corrosiveness, ethanol can cause extensive tissue coagulative necrosis in clinical practice, leading to serious complications such as acute pancreatitis, bleeding, pancreatic duct stricture, abdominal pain, and pancreatic fistula.[47] The incidence of these adverse effects is positively correlated with the injected volume, limiting the use of ethanol. As a result, potential risks must be carefully considered before ablation therapy, especially in cases where advanced tumors require more injections. Polidocanol is generally considered a safe alternative to ethanol.[48] However, there was no statistic difference between the polidocanol (i.t.) group and the NS (i.t.) group (P=0.258) in tumor weight. Due to the excellent biosafety of GEM/PPP hydrogel, it possesses greater clinical applicability than ethanol.

Pathomorphological Examination

The therapeutic effects and biosafety of GEM/PPP hydrogel were further supported by pathological examination. The GEM (i.v.) and (i.t.) group showed obvious extramedullary hematopoiesis and splenic damage (Figure 8A). Hepatic pericentral steatosis was observed in the GEM (i.t.) and ethanol (i.t.) group, indicating liver damage. However, no significant damage to vital organs was observed in the GEM/PPP hydrogel (i.t.) group, confirming its safety profile. Figure 8B revealed varying degrees of tissue necrosis in all treatment groups, with the largest area of necrosis in the GEM/PPP hydrogel (i.t.) group. Moreover, the GEM/PPP hydrogel (i.t.) group exhibited significantly lower numbers of

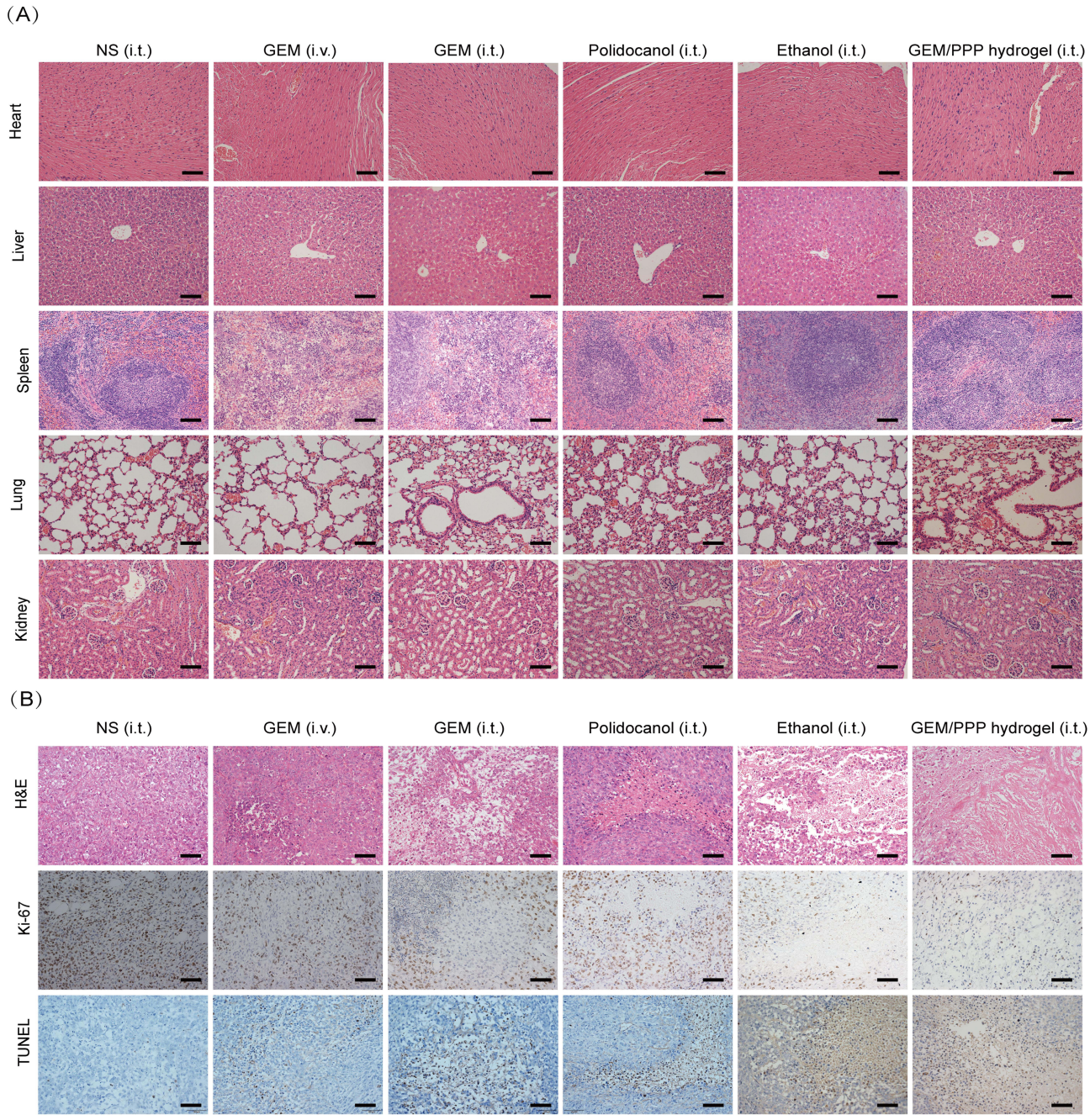

Figure 8 The evaluation of anti-tumor efficacy and systemic toxicity through pathology. (**A**) Representative micrographs of major organs stained by H&E. Splenic hyperplasia was observed in the GEM (i.v.) and (i.t.) group, suggesting extramedullary hematopoiesis and splenic damage. Hepatic pericentral steatosis was observed in the GEM (i.t.) and ethanol (i.t.) group, indicating liver damage. No tissue damage was seen in GEM/PPP hydrogel (i.t.) group. (**B**) Representative micrographs of tumor sections stained by H&E, Ki-67 and TUNEL. Scale bar is 100 μm.

Ki-67 positive cells compared to other groups ($P < 0.001$), while TUNEL staining exhibited the highest positive expression ($P < 0.01$), suggesting minimal malignant proliferation of tumor cells and maximal apoptosis in this group. These results confirmed the superior anti-tumor effect of GEM/PPP hydrogel at the pathological level.

However, our study has some limitations. We lacked experiments on polymer characterization. Additionally, the diffusion range of GEM/PPP during EUS-FNI was not specifically investigated, which is crucial for ensuring proper tumor targeting without damaging surrounding tissues. Further research is needed to assess these aspects, providing additional data and insights for future clinical applications and optimal use of the delivery system.

Conclusion

In summary, we have developed a novel biocompatible hydrogel drug delivery system that enables the sustained delivery of GEM to pancreatic tumors. The injectable and thermo-sensitive GEM/PPP hydrogel developed in this study can be easily administered by fine-needle injection and forms an in situ drug depot triggered by body temperature, offering a novel approach for targeted chemotherapy. In combination with EUS-FNI technology, our drug delivery system overcame challenges such as rapid drug clearance and stromal barriers, promoting significant anti-tumor effects while maintaining safety. Our study demonstrates the potential clinical translation of basic materials and precise targeted chemotherapy. Furthermore, we provide relevant ultrasonographic images that serve as an important reference for future clinical research. Our work highlights the significance of the integration of basic and clinical research, which can bridge the gap between them and facilitate the development of translational medicine.

Ethics Statements

All animal experiments were approved by the Animal Care & Welfare Committee of Guangxi Medical University (Checking number: 202212003) and were conducted in compliance with the Laboratory Animal-Guideline for Ethical Review of Animal Welfare issued by the National Standard GB/T35892-2018 of the People's Republic of China.

Acknowledgments

This work was supported by the National Natural Science Foundation of China [grant number 82260539; 81960439]; and the Project of the Health Department of Guangxi Zhuang Autonomous Region [grant number Z2016322]; and the Guangxi Natural Science Foundation [grant number YYZS2020007].

Disclosure

The authors report no conflicts of interest in this work.

References

1. Mizrahi JD, Surana R, Valle JW, et al. Pancreatic cancer. *Lancet*. 2020;395(10242):2008–2020. doi:10.1016/S0140-6736(20)30974-0
2. Sung H, Ferlay J, Siegel RL, et al. Global Cancer Statistics 2020: GLOBOCAN Estimates of Incidence and Mortality Worldwide for 36 Cancers in 185 Countries. *CA Cancer J Clin*. 2021;71(3):209–249. doi:10.3322/caac.21660
3. Park W, Chawla A, O'Reilly EM. Pancreatic Cancer: a Review. *JAMA*. 2021;326(9):851–862. doi:10.1001/jama.2021.13027
4. Gemenetzis G, Groot VP, Blair AB, et al. Survival in locally advanced pancreatic cancer after neoadjuvant therapy and surgical resection. *Ann Surg*. 2019;270(2):340–347. doi:10.1097/SLA.0000000000002753
5. Ullman NA, Burchard PR, Dunne RF, et al. immunologic strategies in pancreatic cancer: making cold tumors hot. *J Clin Oncol*. 2022;40 (24):2789–2805. doi:10.1200/JCO.21.02616
6. Kukkar D, Kukkar P, Kumar V, et al. Recent advances in nanoscale materials for antibody-based cancer theranostics. *Biosens Bioelectron*. 2020;173:112787. doi:10.1016/j.bios.2020.112787
7. Abdel-Wahab R, Varadhachary GR, Bhosale PR, et al. Randomized, Phase I/II study of gemcitabine plus IGF-1R antagonist (MK-0646) versus gemcitabine plus erlotinib with and without MK-0646 for advanced pancreatic adenocarcinoma. *J Hematol Oncol*. 2018;11(1):71. doi:10.1186/s13045-018-0616-2
8. Miller AL, Garcia PL, Yoon KJ. Developing effective combination therapy for pancreatic cancer: an overview. *Pharmacol Res*. 2020;155:104740. doi:10.1016/j.phrs.2020.104740
9. Reid JM, Qu W, Safgren SL, et al. Phase I trial and pharmacokinetics of gemcitabine in children with advanced solid tumors. *J Clin Oncol*. 2004;22:2445–2451.
10. Tao J, Yang G, Zhou W, et al. Targeting hypoxic tumor microenvironment in pancreatic cancer. *J Hematol Oncol*. 2021;14(1):14. doi:10.1186/s13045-020-01030-w

11. Neesse A, Bauer CA, Öhlund D, et al. Stromal biology and therapy in pancreatic cancer: ready for clinical translation? *Gut*. 2019;68(1):159–171. doi:10.1136/gutjnl-2018-316451
12. Sherman MH, Beatty GL. Tumor Microenvironment in Pancreatic Cancer Pathogenesis and Therapeutic Resistance. *Annu Rev Pathol*. 2023;18:123–148. doi:10.1146/annurev-pathmechdis-031621-024600
13. Liang C, Shi S, Meng Q, et al. Complex roles of the stroma in the intrinsic resistance to gemcitabine in pancreatic cancer: where we are and where we are going. *Exp Mol Med*. 2017;49(12):e406. doi:10.1038/emm.2017.255
14. Funamizu N, Honjo M, Tamura K, et al. microRNAs Associated with Gemcitabine Resistance via EMT, TME, and Drug Metabolism in Pancreatic Cancer. *Cancers*. 2023;15(4):1230. doi:10.3390/cancers15041230
15. Pandit S, Palvai S, Massaro NP, et al. Tissue-reactive drugs enable materials-free local depots. *J Control Release*. 2022;343:142–151. doi:10.1016/j.jconrel.2022.01.023
16. van Roessel S, van Veldhuisen E, Klompmaker S, et al. Evaluation of Adjuvant Chemotherapy in Patients With Resected Pancreatic Cancer After Neoadjuvant FOLFIRINOX Treatment. *JAMA Oncol*. 2020;6(11):1733–1740. doi:10.1001/jamaoncol.2020.3537
17. Timmer FEF, Geboers B, Nieuwenhuizen S, et al. Locally Advanced Pancreatic Cancer: percutaneous Management Using Ablation, Brachytherapy, Intra-arterial Chemotherapy, and Intra-tumoral Immunotherapy. *Curr Oncol Rep*. 2021;23(6):68. doi:10.1007/s11912-021-01057-3
18. Matsumoto K, Kato H. Endoscopic ablation therapy for the pancreatic neoplasms. *Dig Endosc*. 2023;35(4):430–442. doi:10.1111/den.14468
19. Levy MJ, Alberts SR, Bamlet WR, et al. EUS-guided fine-needle injection of gemcitabine for locally advanced and metastatic pancreatic cancer. *Gastrointest Endosc*. 2017;86(1):161–169. doi:10.1016/j.gie.2016.11.014
20. Akhter MH, Rizwanullah M, Ahmad J, et al. Nanocarriers in advanced drug targeting: setting novel paradigm in cancer therapeutics. *Artif Cells Nanomed Biotechnol*. 2018;46(5):873–884. doi:10.1080/21691401.2017.1366333
21. Akhter MH, Kumar S, Nomani S. Sonication tailored enhance cytotoxicity of naringenin nanoparticle in pancreatic cancer: design, optimization, and in vitro studies. *Drug Dev Ind Pharm*. 2020;46(4):659–672. doi:10.1080/03639045.2020.1747485
22. Wei W, Tang J, Li H, et al. Antitumor Effects of Self-Assembling Peptide-Emodin in situ Hydrogels in vitro and in vivo. *Int J Nanomedicine*. 2021;16:47–60. doi:10.2147/IJN.S282154
23. Li W, Zhang L, Ge X, et al. Microfluidic fabrication of microparticles for biomedical applications. *Chem Soc Rev*. 2018;47(15):5646–5683. doi:10.1039/c7cs00263g
24. Mitchell MJ, Billingsley MM, Haley RM, et al. Engineering precision nanoparticles for drug delivery. *Nat Rev Drug Discov*. 2021;20(2):101–124. doi:10.1038/s41573-020-0090-8
25. Chen Q, Wang Q, Wang Y, et al. Penetrating Micelle for Reversing Immunosuppression and Drug Resistance in Pancreatic Cancer Treatment. *Small*. 2022;18(18):e2107712. doi:10.1002/smll.202107712
26. Qian Y, Liu Q, Li P, et al. Highly Tumor-Specific and Long-Acting Iodine-131 Microbeads for Enhanced Treatment of Hepatocellular Carcinoma with Low-Dose Radio-Chemoembolization. *ACS Nano*. 2021;15(2):2933–2946. doi:10.1021/acsnano.0c09122
27. Tang M, Svirskis D, Leung E, et al. Can intracellular drug delivery using hyaluronic acid functionalised pH-sensitive liposomes overcome gemcitabine resistance in pancreatic cancer? *J Control Release*. 2019;305:89–100. doi:10.1016/j.jconrel.2019.05.018
28. Xu H, Paxton JW, Wu Z. Development of Long-Circulating pH-Sensitive Liposomes to Circumvent Gemcitabine Resistance in Pancreatic Cancer Cells. *Pharm Res*. 2016;33(7):1628–1637. doi:10.1007/s11095-016-1902-8
29. Tan B, Huang L, Wu Y, et al. Advances and trends of hydrogel therapy platform in localized tumor treatment: a review. *J Biomed Mater Res A*. 2021;109(4):404–425. doi:10.1002/jbm.a.37062
30. Bordbar-Khiabani A, Gasik M. Smart Hydrogels for Advanced Drug Delivery Systems. *Int J Mol Sci*. 2022;23(7):3665. doi:10.3390/ijms23073665
31. Gao C, Cheng K, Li Y, et al. Injectable Immunotherapeutic Hydrogel Containing RNA-Loaded Lipid Nanoparticles Reshapes Tumor Microenvironment for Pancreatic Cancer Therapy. *Nano Lett*. 2022;22(22):8801–8809. doi:10.1021/acs.nanolett.2c01994
32. Shabana AM, Kambhampati SP, Hsia R-C, et al. Thermosensitive and biodegradable hydrogel encapsulating targeted nanoparticles for the sustained co-delivery of gemcitabine and paclitaxel to pancreatic cancer cells. *Int J Pharm*. 2021;593:120139. doi:10.1016/j.ijpharm.2020.120139
33. Shi K, Xue B, Jia Y, et al. Sustained co-delivery of gemcitabine and cis-platinum via biodegradable thermo-sensitive hydrogel for synergistic combination therapy of pancreatic cancer. *Nano Res*. 2019;12(6):1389–1399. doi:10.1007/s12274-019-2342-7
34. Lakhtakia S, Seo D-W. Endoscopic ultrasonography-guided tumor ablation. *Dig Endosc*. 2017;29(4):486–494. doi:10.1111/den.12833
35. Jing Z, Ni R, Wang J, et al. Practical strategy to construct anti-osteosarcoma bone substitutes by loading cisplatin into 3D-printed titanium alloy implants using a thermosensitive hydrogel. *Bioact Mater*. 2021;6(12):4542–4557. doi:10.1016/j.bioactmat.2021.05.007
36. Chan PS, Xian JW, Li Q, et al. Biodegradable Thermosensitive PLGA-PEG-PLGA Polymer for Non-irritating and Sustained Ophthalmic Drug Delivery. *AAPS J*. 2019;21(4):59. doi:10.1208/s12248-019-0326-x
37. Chen X, Wang M, Yang X, et al. Injectable hydrogels for the sustained delivery of a HER2-targeted antibody for preventing local relapse of HER2+ breast cancer after breast-conserving surgery. *Theranostics*. 2019;9(21):6080–6098. doi:10.7150/thno.36514
38. Kremenovic M, Chan AA, Feng B, et al. BCG hydrogel promotes CTSS-mediated antigen processing and presentation, thereby suppressing metastasis and prolonging survival in melanoma. *J Immunother Cancer*. 2022;10(6):e004133. doi:10.1136/jitc-2021-004133
39. Rahmani F, Atabaki R, Behrouzi S, et al. The recent advancement in the PLGA-based thermo-sensitive hydrogel for smart drug delivery. *Int J Pharm*. 2023;631:122484. doi:10.1016/j.ijpharm.2022.122484
40. Garner J, Davidson D, Eckert GJ, et al. Reshapable polymeric hydrogel for controlled soft-tissue expansion: in vitro and in vivo evaluation. *J Control Release*. 2017;262:201–211. doi:10.1016/j.jconrel.2017.07.029
41. Williams DF. The plasticity of biocompatibility. *Biomaterials*. 2023;296:122077. doi:10.1016/j.biomaterials.2023.122077
42. Mellati A, Hasanzadeh E, Gholipourmalekabadi M, et al. Injectable nanocomposite hydrogels as an emerging platform for biomedical applications: a review. *Mater Sci Eng C Mater Biol Appl*. 2021;131:112489. doi:10.1016/j.msec.2021.112489
43. Andersen HB, Ialchina R, Pedersen SF, et al. Metabolic reprogramming by driver mutation-tumor microenvironment interplay in pancreatic cancer: new therapeutic targets. *Cancer Metastasis Rev*. 2021;40(4):1093–1114. doi:10.1007/s10555-021-10004-4
44. Chyzy A, Tomczykowa M, Plonska-Brzezinska ME. Hydrogels as potential nano-, micro- and macro-scale systems for controlled drug delivery. *Materials*. 2020;13(1):188. doi:10.3390/ma13010188
45. Cai H, Wang R, Guo X, et al. Combining Gemcitabine-Loaded Macrophage-like Nanoparticles and Erlotinib for Pancreatic Cancer Therapy. *Mol Pharm*. 2021;18(7):2495–2506. doi:10.1021/acs.molpharmaceut.0c01225

46. Saghir SM, Dhindsa BS, Daid SGS, et al. Safety and efficacy of EUS-guided ablation of pancreatic lesions with ethanol versus ethanol with paclitaxel: a systematic review and meta-analysis. *Endosc Ultrasound*. 2022;11(5):371–376. doi:10.4103/EUS-D-20-00185
47. Rimbaş M, Horumbă M, Rizzatti G, et al. Interventional endoscopic ultrasound for pancreatic neuroendocrine neoplasms. *Dig Endosc*. 2020;32(7):1031–1041. doi:10.1111/den.13635
48. Wijnands TF, Schoenemeier B, Potthoff A, et al. Ethanol sclerotherapy or polidocanol sclerotherapy for symptomatic hepatic cysts. *United Eur Gastroenterol J*. 2018;6(6):919–925. doi:10.1177/2050640618764940